Ultrasonic shear wave properties of soft tissues and tissuelike materials

Ernest L. Madsen
Departments of Medical Physics and Radiology, University of Wisconsin, Madison, Wisconsin 53706

H. John Sathoff
Department of Physics, Bradley University, Peoria, Illinois 61625

James A. Zagzebski
Departments of Medical Physics and Radiology, University of Wisconsin, Madison, Wisconsin 53706

(Received 24 March 1983; accepted for publication 26 July 1983)

Determinations of shear wave speeds of sound and attenuation coefficients are reported for soft tissues, a silicone rubber reference material, and a gel used in manufacturing ultrasonically tissue-mimicking materials. Fresh bovine tissues were investigated, including calfskin, liver, cardiac muscle, and striated muscle. Because of the very large shear wave attenuation coefficients, reasonably accurate determinations of shear wave properties are difficult to make. The quantity measured directly was the complex reflection coefficient for shear waves at a planar interface between the sample and fused silica. Measurements were made at frequencies spanning the range 2–14 MHz. The shear wave attenuation coefficients increase with frequency and are of the order of 10^4 times the longitudinal wave attenuation coefficients. The shear wave speeds of sound also increase with frequency but are only a few percent of the longitudinal wave speeds of sound. The results are accurate enough to allow frequency dependencies to be proposed.

PACS numbers: 43.80.Cs, 43.35.Cg

INTRODUCTION

At present, the important clinical means of transmission of ultrasonic energy, both for diagnostic and therapeutic purposes, occurs via compressional, or longitudinal, waves. Many aspects of the interaction of ultrasonic waves with tissues are not completely understood. For example, it appears that a significant fraction of the attenuation of longitudinal waves in soft tissues involves proteins at the macromolecular scale [1–3]; just what fraction this is remains open to question.[3]

Another process which may contribute significantly to longitudinal wave attenuation in soft tissues consists of mode conversion at interfaces involving abrupt changes in density and/or compressibility. Interfaces involved may be of the order of a micron in diameter. (This is also referred to as "viscous relative motion.")[4,5] Theoretical models for this attenuation process were developed by Epstein and Carhart[6] and extended by Allegra and Hawley.[7] These models have been applied to a microscopic soft tissue model by O'Donnell and Miller.[5] To facilitate computations in the latter tissue model, estimates were made by the authors regarding numerical values of many relevant physical properties including the shear wave properties of the media involved.

We have measured values for the shear wave speeds of sound and attenuation coefficients for bulk tissue parenchymae. It may develop that knowledge of such values and their frequency dependencies will facilitate gaining insight at the microscopic level regarding the involvement of shear waves in longitudinal wave attenuation in soft tissues.

We have also measured these shear wave properties for a water-based, animal-hide gel which is employed in the manufacture of ultrasonically tissue-mimicking (TM) materials.[8] In producing these TM materials, microscopic solid or liquid particles are suspended in the gel; the longitudinal attenuation coefficients of the resulting materials exhibit a proportionality to frequency as is the case for many tissues. The slope of the attenuation coefficient plotted versus frequency increases with the concentration of the particles.

One motivation for determining the shear wave properties of this gel was to obtain information that could be used in applying the theory mentioned above[6,7] to see if it can explain the longitudinal attenuation properties of the TM materials. The comparison of theory with experiment for these TM materials is the subject of another paper.

Extensive investigations of complex shear wave impedances in viscous nonbiological liquids have been made by Lamb and associates.[9–11] Shear wave speeds of sound and attenuation coefficients can be calculated from these complex shear wave impedances.

Measurements of shear wave speeds of sound and attenuation coefficients are difficult to make for soft tissues and tissuelike media (as well as for viscous liquids) because of the extremely large values of the shear wave attenuation coefficients involved. Frizzell[12,13] has made measurements of these properties for a few tissues and reference materials. For soft tissues, Frizzell obtained values for shear wave attenuation coefficients of the order of 10 000 times those for longitudinal waves. Shear wave speeds of sound were in the area of 50 m/s. In some cases the standard deviations were of the order of the quantities measured. Also, except for the case of homogenized liver, measurements were done at no more than two frequencies on any single type of tissue or other nonliquid material. For homogenized liver, measurements were made at three frequencies, but standard deviations in the data were so large that estimations of frequency depen-

 0001-4966/83/111346-10$00.80 © 1983 Acoustical Society of America

dencies of shear wave parameters were precluded here also.

In this report data on shear wave properties are given for various bovine soft tissue parenchymae, for tissuelike media, and for RTV 615[14] (also used as a reference material by Frizzell). For each material the shear wave speeds of sound and attenuation coefficients were determined at about ten different frequencies between 2.5 and 14.0 MHz. The tissuelike materials included the water-based gel used in making ultrasonically tissue-mimicking (TM) materials, and a version of ultrasonically tissue-mimicking liver.[8]

The quantity measured, from which the two shear wave properties can be determined, is the complex reflection coefficient R, for shear waves at the interface between the material of concern and an optically flat fused silica surface. The precision of our measurements appears to be about the same as Frizzell's at any one frequency; however, because of the large number of frequencies used in the present study, statements regarding frequency dependencies of the shear wave properties can be made.

I. THEORETICAL REVIEW CONNECTING THE COMPLEX REFLECTION COEFFICIENT WITH SHEAR WAVE PROPERTIES

A brief review of relevant theoretical relationships are given below. The Voigt model of a viscoelastic material is employed.

A. The one-dimensional shear wave equation with a complex shear modulus

For a lossless isotropic medium, and neglecting higher order terms, the one-dimensional wave equation for shear wave propagation in the x direction is

$$\mu_1 \frac{\partial^2 y}{\partial x^2} = \rho \frac{\partial^2 y}{\partial t^2}.$$

Here y is the particle displacement (perpendicular to the direction of propagation), t is the time, and ρ is the density of the medium. The constant μ_1 is the (static) shear modulus of the medium[15]; it equals $(F/A)/(\Delta y/\Delta x)$, where F is the magnitude of each force forming a shearing couple applied tangentially to parallel surfaces of area A and separation Δx, while Δy is the tangential displacement from equilibrium of these surfaces relative to one another in response to application of the couple. A dynamic component of the shear modulus can be defined as

$$\mu_2 = (F/A)/(\Delta \dot{y}/\Delta x),$$

where quantities are defined above except Δy has been replaced by $\Delta \dot{y}$ which is the change in particle velocity over the distance Δx. The constant μ_2 is more commonly referred to as the coefficient of viscosity. In the derivation of the linearized shear wave equation the relation

$$\frac{\partial (F/A)}{\partial x} = \frac{\partial}{\partial x}\left(\mu_1 \frac{\Delta y}{\Delta x} + \mu_2 \frac{\Delta \dot{y}}{\Delta x}\right)$$

is employed on one side of the equation. We have $\Delta \dot{y} = -i\omega \Delta y$ for a sinusoidal time dependence of the shear waves embodied in the factor $e^{-i\omega t}$; therefore, a complex shear modulus can be defined as $\mu \equiv \mu_1 - i\omega_2$, and the wave equation remains in the usual form

$$\mu \frac{\partial^2 y}{\partial x^2} = \rho \frac{\partial^2 y}{\partial t^2}. \tag{1}$$

An analogous discussion appears in Ref. 12. Notice that this discussion applies for a time factor of $e^{-i\omega t}$, not for the alternative, $e^{+i\omega t}$.

B. The complex reflection coefficient and its relation to the shear wave speed of sound and attenuation coefficient

Consider a plane sinusoidal shear wave normally incident on a planar interface between two different homogeneous media (see Fig. 1). Let A_o, A_r, and A_T be the (real, positive) displacement amplitudes of the incident, reflected, and transmitted plane waves. Also, let $x = 0$ at the planar interface.

Define

$$y_0 \equiv A_0 e^{i(k_a x - \omega t)},$$

for the incident wave,

$$y_r \equiv A_r e^{i(-k_a x - \omega t + \phi_r)},$$

for the reflected wave, and

$$y_T \equiv A_T e^{i(k_b x - \omega t + \phi_T)},$$

for the transmitted wave. Here ϕ_r and ϕ_T are phase constants determined by the boundary conditions, and k_a and k_b are the (complex) wavenumbers in media a and b, respectively. Each of y_0, y_r and y_T must satisfy the wave equation given in Eq. (1) above.

This means that

$$\mu_a = \omega^2 \rho_a / k_a^2 \tag{2}$$

and

$$\mu_b = \omega^2 \rho_b / k_b^2 \tag{3}$$

where μ_a and μ_b are the complex shear moduli in media a and b, respectively, and ρ_a and ρ_b are the simple (real) mass densities of media a and b. These densities are constant for the small amplitude shear waves considered.

The boundary conditions to be satisfied are that the net amplitude and shear stress are each continuous across the

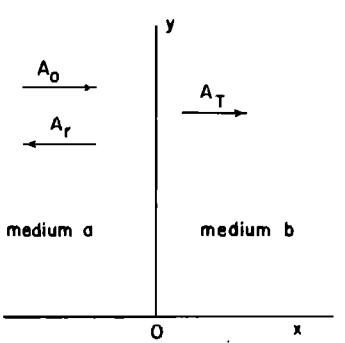

FIG. 1. Diagram to aid in the discussion of the relation between the complex reflection coefficient and shear wave properties. The arrows describe directions of propagation of plane sinusoidal shear waves; these directions are perpendicular to the planar interface between media a and b.

interface. This assumes that no sliding occurs between the two media precisely at the interface.

Thus

$$y_0 + y_r = y_T \quad \text{at } x = 0$$

and

$$\mu_a \frac{\partial (y_0 + y_r)}{\partial x}\bigg|_{x=0} = \mu_b \frac{\partial y_T}{\partial x}\bigg|_{x=0}.$$

Thus we have at $x = 0$,

$$A_0 + A_r e^{i\phi_r} = A_T e^{i\phi_T} \tag{4}$$

and

$$\mu_a \{A_0 i k_a - A_r i k_a e^{i\phi_r}\} = \mu_b A_T i k_b e^{i\phi_T}. \tag{5}$$

The complex amplitude reflection coefficient is defined as

$$R \equiv \frac{y_r}{y_0}\bigg|_{x=0} = \frac{A_r e^{i\phi_r}}{A_0}.$$

Thus the modulus of R is given by

$$\|R\| = A_r/A_0$$

and its phase angle is ϕ_r.

Equations (4) and (5) can now be solved for R:

$$R = (\mu_a k_a - \mu_b k_b)/(\mu_a k_a + \mu_b k_b).$$

Using relations (2) and (3), we have

$$R = (\rho_a k_b - \rho_b k_a)/(\rho_a k_b + \rho_b k_a). \tag{6}$$

If medium a is a solid and medium b is a vacuum (or a near approximation such as air), the right-hand side of Eq. (5) is zero since medium b cannot support a shear stress. Thus, the quantity in curly braces on the left side is zero which requires R to be 1 for this case.

The complex wavenumber k, contains the shear wave speed of sound c, and attenuation coefficient α, in the form

$$k = \omega/c + i\alpha.$$

If R, ρ_a, ρ_b, and k_a are known, Eq. (6) can be solved for c_b and α_b. The solution for c_b is

$$c_b = 2A\omega/[-B + (B^2 - 4AC)^{1/2}], \tag{7}$$

where

$$A \equiv 1 + \left(\frac{1 + R^*R}{1 - R^*R}\right)^2 \tan^2\phi_r,$$

$$B \equiv -2\frac{\rho_b k_a}{\rho_a}\left(\frac{1 + R^*R}{1 - R^*R}\right)(1 + \tan^2\phi_r),$$

and

$$C \equiv (\rho_b k_a/\rho_a)^2 (1 + \tan^2\phi_r).$$

R^* refers to the complex conjugate of R. The solution for α_b can be expressed in terms of c_b as follows:

$$\alpha_b = \left[-\frac{\omega^2}{c_b^2} + 2\frac{\rho_b k_a}{\rho_a}\left(\frac{1 + R^*R}{1 - R^*R}\right)\frac{\omega}{c_b} - \left(\frac{\rho_b k_a}{\rho^a}\right)^2\right]^{1/2}. \tag{8}$$

Thus knowing the densities of media a and b and the shear wave speed of sound and attenuation coefficient for material a (determining k_a), then determination of the modulus, $\|R\| = (R^*R)^{1/2}$, and phase angle ϕ_r, of the complex reflection coefficient allows calculation of the shear wave speed of sound and attenuation coefficient for material b at angular frequency ω.

II. METHODS OF MEASUREMENT OF THE COMPLEX REFLECTION COEFFICIENT R

A. The main concepts

A diagram of the experimental apparatus is shown in Fig. 2. Longitudinal narrowband pulses, also referred to as continuous wave (cw) bursts, are generated by transducer A. This transducer is coupled via petroleum jelly to one of the flat surfaces of a mode conversion block. The geometry of the block is such that the angle between the transducer axis and the first reflecting surface r, equals the angle of incidence such that incident longitudinal waves are converted completely into shear waves within the fused silica assuming no sound energy is transmitted into the air at this surface.[16] The 137.3° angle shown on the mode conversion block is the supplementary angle for this angle of incidence. The surface S of the mode conversion block at which the reflection coefficient is measured is that horizontal surface immediately beneath the "sample" in the figure. The orientation of the surface S is such that the shear waves emerging from surface r have a 90° angle of incidence relative to that surface.

This surface is also referred to as the "stage" in this article. The cw pulse reflected at surface S returns to surface r where it is converted back into the longitudinal mode upon reflection. This longitudinal cw pulse then returns to the surface of the block to which transducer A is applied, an echo is observed through that transducer, and part of the returning wave is reflected. The longitudinal cw wave re-

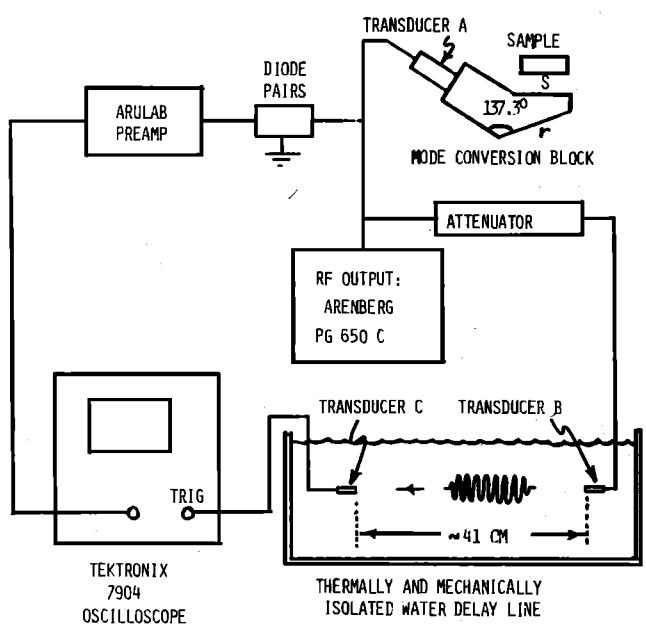

FIG. 2. Diagram of the experimental apparatus. The sample is shown above the stage S, which is one of the flat surfaces on the fused silica mode conversation block. Transducers A and B emit cw pulses simultaneously.

flected at the surface to which transducer A is applied then initiates a second cycle consisting of the same four steps. This process repeats again and again, the echo signals at transducer A becoming continually weaker primarily because of energy being delivered to the transducer during reflection at its surface. A reasonably strong echo still exists for the tenth echo and beyond, however.

At the same time that the initial pulse is introduced into the block by transducer A, a time reference pulse is emitted by transducer B in a thermally and mechanically isolated delay line. The oscilloscope is externally triggered by the time delayed signal delivered by receiving transducer C in the water path delay line. The distance between transducers B and C is adjusted so that part of the tenth echo received by receiver A is displayed on the oscilloscope.

When a sample, the shear wave properties of which are to be measured, is pressed onto the stage (or surface S) of the mode conversion block, the air is displaced by the sample and the reflection coefficient at S changes. A decrease in amplitude of the echoes occurs and also the phases shift slightly. The phase shift observed for the tenth echo is ten times that for a single reflection. In terms of time shifts, the total phase shifts observed were of the order of a nanosecond. The smallness of this shift is one reason for observing the tenth echo rather than, say, the second. The ratio of the amplitude of tenth echo with the sample in contact with the stage to the amplitude in its absence is the tenth power of that when only one reflection occurs at the surface S. Knowledge of the phase shift and amplitude ratio allows calculation of the shear wave ultrasonic properties consisting of the speed of sound and attenuation coefficient. Details of this procedure are given in Sec. I.

B. Details involving data acquisition

As implied in the last paragraph, there were two directly measured quantities for each material and each frequency considered. All measurements were made involving the tenth echo received by transducer A, and all were made by direct observation of the echo voltage wave form displayed on the oscilloscope. First, the ratio of the echo voltage amplitude with the sample impressed on the stage to that in the absence of the sample was determined. About five measurements of this ratio were made for each sample and each frequency. The sample was reapplied to the stage for each of these measurements. Second, the phase shift occurring when the air above the stage was displaced by the sample was measured. For both cases, data were recorded first using the wave form when air only existed above the stage (surface S in Fig. 2) and then with the sample impressed onto the stage. The reason for this ordering was to aid in minimizing thermal effects at the stage. (The speed of sound in fused silica varies significantly with temperature.) Before each measurement, the stage was cleaned with ethyl alcohol, dried, and allowed to reach thermal equilibrium the latter being determined by the stability of the wave form on the oscilloscope. For each sample and frequency, measurements for six to ten applications were recorded to determine the phase shift. Except for a calfskin sample, each sample was a rectangular parallelpiped about 1.5 cm thick having two opposite sides with areas slightly less than the area of the stage. The calfskin consisted of a rectangular layer which was wrapped onto an appropriately shaped piece of Lucite.[17] All samples were kept between two stainless steel slabs between successive impressments onto the stage so that they remained at room temperature (23° C $\pm$ 1° C).

C. Key components of the measurement apparatus

1. The water path delay line

A major factor in producing adequate precision for the measurements is the high degree of stability of the water path delay line. For this apparatus the water path length required was about 41cm. For a speed of sound in water at 22° C of 1489 m/s and a temperature coefficient (5m/s)/°C, a temperature shift of $\frac{5}{10\,000}$° C can produce a shift in the trigger delay time of $\frac{1}{2}$ ns. This shift is of the order of the time shifts that must be measured in determining the reflection coefficient. This same shift in delay time occurs if the distance between the transmitter B and receiver C changes by 0.75 μ due to some external mechanical disturbance such as might be caused by a nearby motor. Therefore, considerable effort was devoted to producing thermal and mechanical isolation. A water tank was surrounded by 2.5-cm-thick layers of Styrofoam,[18] and a Saran Wrap layer was applied to the top of the water tank to reduce air convection currents. The water tank sat in a large box of sand weighing several hundred pounds, and the box was supported by four inflated inner tubes.

2. Material for reduction of spurious echoes

Of the eight planar surfaces forming the shape of the mode conversation block, all but three were coated with an ultrasound absorbing material, the acoustic impedance of which must be reasonably close to that of the fused silica. This absorbing material consisted of a mixture of tungsten carbide powder in petroleum jelly. The concentration of powder was a maximum such that the mixture remained air-free (as observed with the naked eye) and would adhere to the appropriate surfaces of the mode conversion block when applied with a spatula. Spurious interfering echoes involving reflections from surfaces of the block other than r, S, or that to which the transducer was applied, all but disappeared following application of this absorbing material.

3. The transducers

Nine different nonfocused transducers were used. These ranged from a 2.54-cm-diam nominal 2.25-mHz transducer to a 0.635-cm-diam nominal 10-MHz transducer.

III. DATA REDUCTION

The changes in net amplitude and phase observed for the tenth echo are due only to the change in complex reflection coefficient at the stage when air is displaced by the sample. The reflection coefficient when air only exists above the stage is 1 (unity) as shown in Sec. IB. When the sample is in

TABLE I. Choices of shear modulus (μ_1) and coefficients of viscosity (μ_2) giving a best fit to the data employing the Voigt model. The dashed curves in Figs. 3–14 correspond to the Voight model using these values for the various types of materials. Mass densities for the various materials are also given.

Material	$\mu_1\left(\frac{\text{dyn}}{\text{cm}^2}\right)$	$\mu_2\left(\frac{\text{dyn-s}}{\text{cm}^2}\right)$	Density $\left(\frac{\text{g}}{\text{cm}^3}\right)$
RTV 615	4.31×10^7	1.49	1.02
calfskin	4.04×10^7	1.31	1.07[a]
striated muscle	0.242×10^7	0.141	1.08
cardiac muscle	0.124×10^7	0.159	1.08
liver	0.0023×10^7	0.127	1.07
animal-hide gel (no particles)	0.190×10^7	0.186	1.02
tissue-mimicking liver (with graphite	...	...	1.06

[a] Value for bovine liver used as an estimate.

place, it is $R \equiv \|R\| e^{i\phi_r}$, where $\|R\| \equiv (R^* R)^{1/2}$. The ratio of observed amplitudes, with and without the sample impressed, is then $\|R\|^{10}$ and the observed phase shift is $10\,\phi_r$. Calculation of the shear wave speed of sound and attenuation coefficient can be done using Eqs. (7) and (8) of Sec. II. For these measurements, medium a in Eqs. (7) and (8) is fused silica and medium b is the sample material. The density of fused silica is $\rho_a = 2.2 \text{g/cm}^3$.[19] The wavenumber for fused silica can be taken to be real (see Ref. 12, p. 45); i.e., the shear wave attenuation coefficient is negligible in these measurements. Thus $k_a = \omega/c_a$, where $c_a = 3764$ m/s is the shear wave speed of sound at room temperature in fused silica.[16] The frequency dependence of the shear wave speed of sound in fused silica is negligible.[20] The density ρ_b is that for the sample material measured. ρ_b for the various materials are listed in Table I. These sample densities were determined in a direct way by measurements of mass and corresponding water volume displacement.[21]

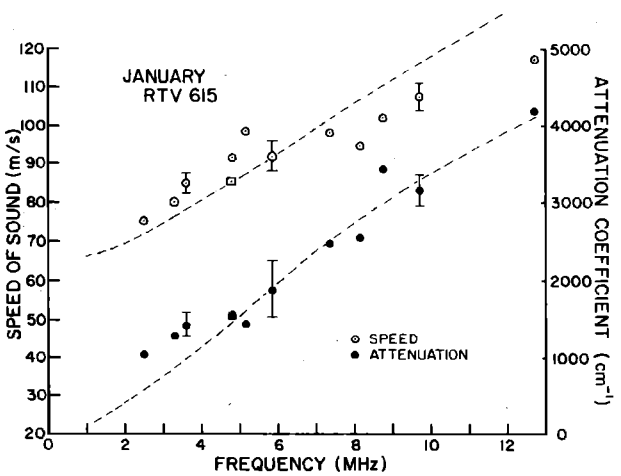

FIG. 3. Shear wave speeds of sound for RTV 615 (open circles ○, and one open square, □) and attenuation coefficients (closed circles ●, and one closed square ■) for various frequencies. The data were obtained during the first period of measurement. The squares correspond to a repeat measurement at 4.80 MHz to test reproducibility; the closed square is superimposed on a closed circle. The dashed lines correspond to the Voigt model for μ_1 and μ_2 given in Table I.

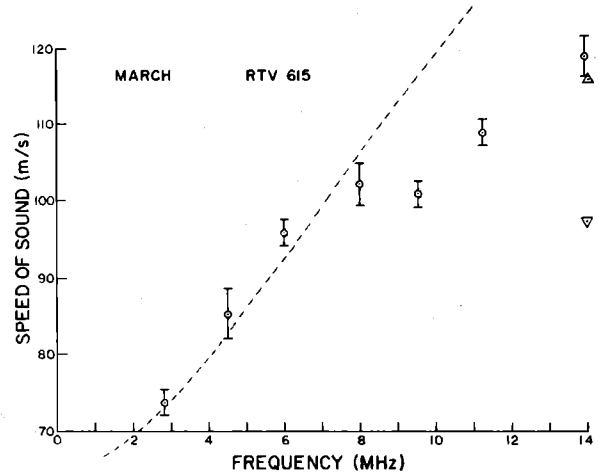

FIG. 4. Shear wave speeds of sound for RTV 615 (open circles, ○) for various frequencies determined during the second period of measurement. The points in the triangles are from Frizzell,[9] the highest value (△) having been obtained using RTV 615 which had solidified while on the measurement stage. The dashed line corresponds to the Voigt model for μ_1 and μ_2 given in Table I.

IV. RESULTS AND ERROR ANALYSIS

The results of this study are shown in Figs. 3–15. In each of these figures, mean values for shear wave speeds of sound c_s, and/or shear wave attenuation coefficients α_s, are plotted for frequencies spanning the range 2–14 MHz. The mean values of attenuation coefficients are plotted as filled-in circles (and in one case a filled-in square), and mean values for speeds of sound are shown in open circles (and in one case an open square). Each mean value was determined by first calculating the mean values of the amplitude ratio and phase shift (see Sec. IIB) and then using these to determine c_s and α_s via Eqs. (7) and (8) of Sec. IB.

Each set of data was obtained during one of two measurement periods, each period lasting a few days. One measurement period followed the other by about two months. Of importance regarding reproducibility considerations, measurements on the reference material RTV 615 were done during both measurement periods, and the results are shown

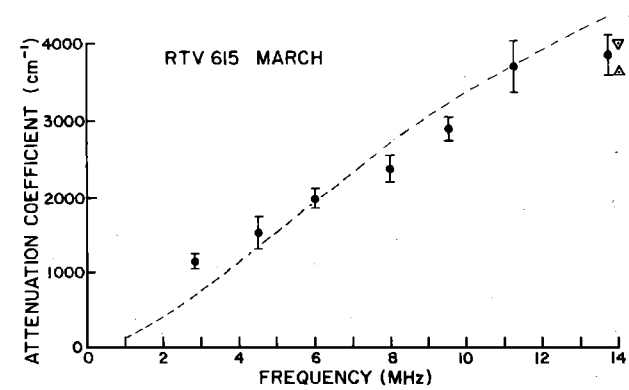

FIG. 5. Shear wave attenuation coefficients for RTV 615 (closed circles, ●) for various frequencies determined during the second period of measurement. The points in triangles are from Frizzell, one of them (△) corresponding to RTV 615 which solidified while on the measurement stage. The dashed line corresponds to the Voigt model for μ_1 and μ_2 given in Table I.

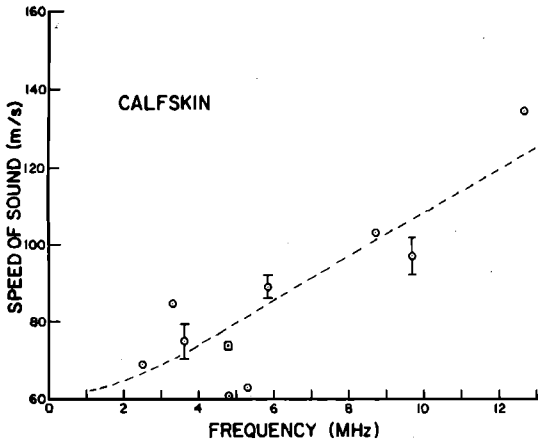

FIG. 6. Shear wave speeds of sound for calfskin (open circles, O) for various frequencies. The point in the square (⊡) resulted from a repeat measurement at 4.80 MHz. The dashed curve corresponds to the Voigt model for values of μ_1 and μ_2 given in Table I.

in Figs. 3–5. Measurements on calfskin (Figs. 6 and 7) and gelatin-based tissuelike materials (Figs. 14 and 15) were done during the earlier period, and measurements on bovine liver, cardiac muscle, and striated muscle were done during the later period; results of the latter are shown in Figs. 8–13.

The error bar associated with any plotted mean value corresponds to the standard deviation. Error bars were determined by the usual propagation of error analysis.[22] First, for a given frequency and material under study, the standard deviations of the magnitude of the reflection coefficient $\|R\|$, and of the phase shift ϕ_r, were found; call these $\sigma_{\|R\|}$ and σ_{ϕ_r}. Then, using Eqs. (4) and (5), $\partial\alpha_s/\partial\|R\|, \partial\sigma_s/\partial\phi_r, \partial c_s/\partial\|R\|$, and $\partial c_s/\partial\phi_r$ were computed where the subscript b has been replaced with s everywhere. The standard deviations of c_s and α_α are then given by

$$\sigma_{c_s} = \left[\left(\frac{\partial c_s}{\partial\|R\|}\right)^2 \sigma^2_{\|R\|} + \left(\frac{\partial c_s}{\partial\phi_r}\right)^2 \sigma^2_{\phi_r}\right]^{1/2}$$

and

$$\sigma_{\alpha_s} = \left[\left(\frac{\partial \alpha_s}{\partial\|R\|}\right)^2 \sigma^2_{\|R\|} + \left(\frac{\partial \alpha_s}{\partial\phi_r}\right)^2 \sigma^2_{\phi_r}\right]^{1/2}.$$

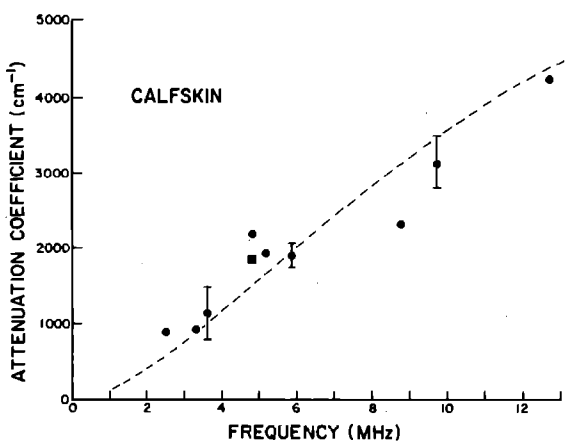

FIG. 7. Shear wave attenuation coefficients for calfskin (closed circles, ●) for various frequencies. The point in the closed square (■) resulted from a repeat measurement at 4.80 MHz. The dashed curve corresponds to the Voigt model for values of μ_1 and μ_2 given in Table I.

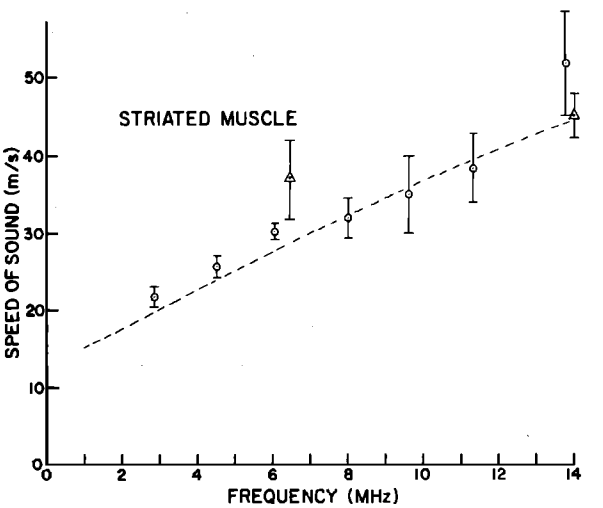

FIG. 8. Shear wave speeds of sound for bovine striated muscle (open circles, O) for various frequencies. The points in triangles (△) are from Frizzell for canine striated muscle. The dashed curve corresponds to the Voigt model for values of μ_1 and μ_2 given in Table I.

V. DISCUSSION

A. Reproducibility of measurements

Figure 3 shows measurements for speeds of sound and attenuation coefficients made on RTV 615 during the first measurement period. Figures 4 and 5 show measurments of speeds of sound and attenuation coefficients, respectively, made on RTV 615 during the second period of measurements (two months later). Excellent reproducibility is demonstrated; allowing for the degree of scatter of data points, the results for one period of measurement are indistinguishable from those for the other period.

Each data point represents a mean value corresponding to many separate applications of the interrogated material onto the "stage." These are highly reproducible measurements; the error bars in Figs. 3–15 represent simple standard deviations of the measured values. Error bars corresponding to the standard deviations of the *means*[23] would be about half the lengths displayed in the figures. Thus the scatter in the data points shown in the figures, particularly for speeds of sound, does not appear to be primarily dependent on the method of application to the stage of the samples.

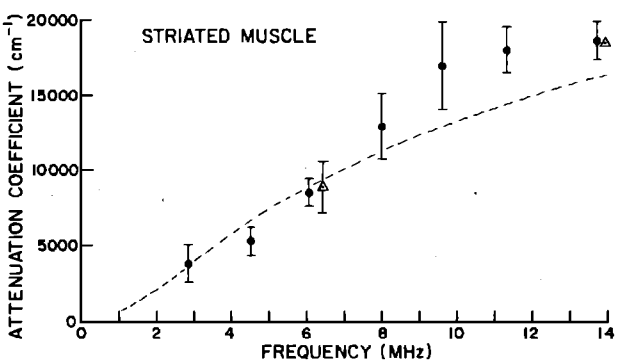

FIG. 9. Shear wave attenuation coefficients for bovine striated muscle (closed circles, ●) for various frequencies. The points in trianges (△) are from Frizzell[9] for canine striated muscle. The dashed curve correspond to the Voigt model for values of μ_1 and μ_2 given in Table I.

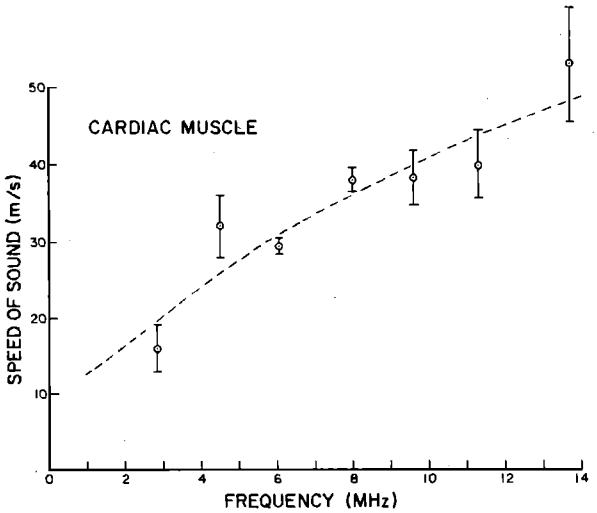

FIG. 10. Shear wave speeds of sound for bovine cardiac muscle (open circles, O) for various frequencies. The dashed curve corresponds to the Voigt model for values of μ_1 and μ_2 given in Table I.

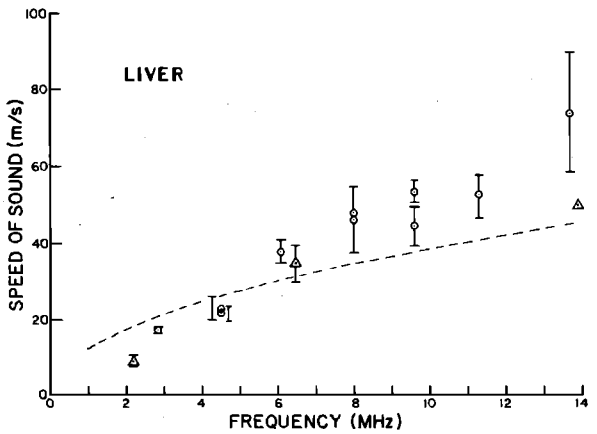

FIG. 12. Shear wave speeds of sound for bovine liver (open circles, O) for various frequencies. The points in triangles are from Frizzell,[9] that at 14 MHz corresponding to rat liver and those at 2.2 and 6.5 MHz to canine liver. The dashed curve corresponds to the Voigt model for values of μ_1 and μ_2 given in Table I.

To gain more insight into the causes of the scatter in the data, two sets of measurements at the frequency 4.80 MHz were made on RTV 615, calfskin, and the tissuelike media during the first measurement period; in the repeated set the source transducer (transmitter A in Fig. 1) was removed from the mode conversion block and then reapplied. The mean value of the speed of sound in RTV 615 obtained in the repeated set of measurements is shown in Fig. 3 in the open square. The data point from the repeated measurement is about 7 m/s lower than that from the previous measurement. The mean value for the attenuation coefficient obtained in the repeated measurements was slightly lower than—but almost identical to—the formerly obtained value; it is plotted as a closed (filled-in) square superimposed on the closed circle in Fig. 3.

Without moving transducer A following the repeat measurements on RTV 615, repeat measurements were also done at 4.80 MHz on calfskin and on the tissuelike materials. The repeat values are shown in Figs. 6, 7, 14, and 15; again the speeds of sound resulting from the repeat measurements are shown as open squares in these figures, and the corresponding attenuation coefficients are shown as closed, or filled-in, squares. The positions of the various repeat data points can be seen to be consistent with the scatter of data points over the various frequencies. In Table II the values for speeds of sound and attenuation coefficients for the repeated measurements and the original measurements are displayed. The percent changes in Table II do not demonstrate a consistent rise or fall for either speeds of sound or attenuation coefficients. For some reason, however, there is a tendency for both the speeds of sound and attenuation coefficients to be higher in the repeat set.

B. Comparison with Frizzell's results

Both we and Frizzell made measurements on RTV 615. In the case of soft tissues, however, our measurements were made on bovine tissues and Frizzell's on canine or rat tissues. Nevertheless, the extent of agreement is still very good for tissues as well as for RTV 615.

Mean values for the real and imaginary parts of the shear acoustic impedance for RTV 615 are given for 14 MHz

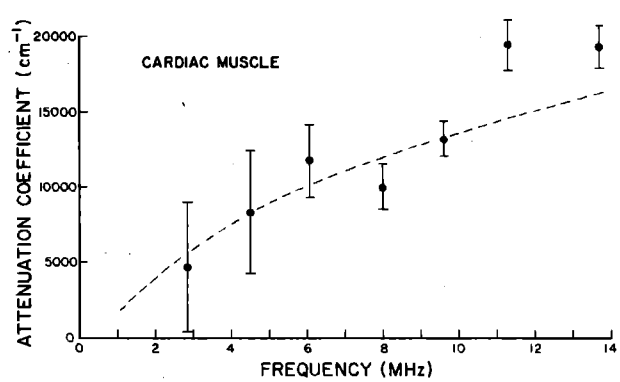

FIG. 11. Shear wave attenuation coefficients for bovine cardiac muscle (closed circles, ●) for various frequencies. The dashed curve corresponds to the Voigt model for values of μ_1 and μ_2 given in Table I.

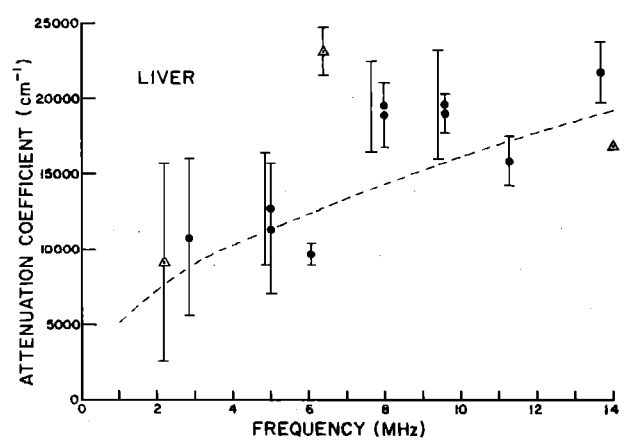

FIG. 13. Shear wave attenuation coefficients for bovine liver (closed circles, ●) for various frequencies. The points in triangles (△) are from Frizzell, that at 14 MHz corresponding to rat liver and those at 2.2 and 6.5 MHz to canine liver. The dashed curve corresponds to the Voigt model for values of μ_1 and μ_2 given in Table I.

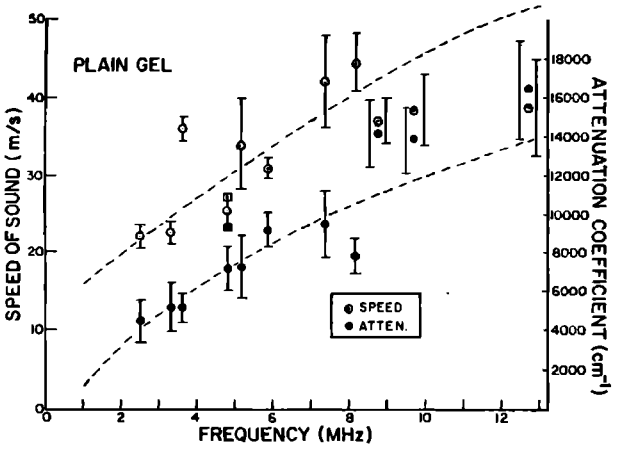

FIG. 14. Shear wave speeds of sound (open circles, O) and attenuation coefficients (closed circles, ●) for the plain animal-hide gel used in the manufacture of ultrasonically tissue-mimicking materials. The point in the open square (⊡) corresponds to a repeat measurement of speed of sound and the points in the closed square (■) corresponds to a repeat measurement of attenuation coefficient. The dashed curves correspond to the Voigt model for values of μ_1 and μ_2 given in Table I.

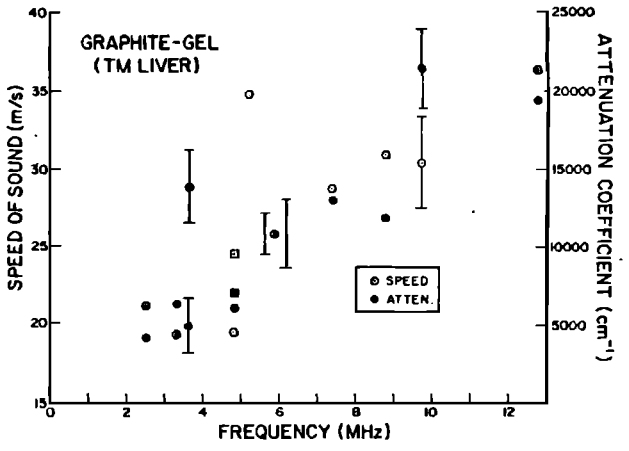

FIG. 15. Shear wave speeds of sound (open circles, O) and attenuation coefficients (closed circles, ●) for tissue-mimicking liver. The points in the open square (⊡) and the closed square (■) correspond to repeat measurements of the speed of sound and attenuation coefficient, respectively, at 4.80 MHz.

by Frizzell. (See Ref. 12, p. 61.) Values for shear wave speeds of sound and attenuation coefficients can be calculated from these. Frizzell made measurements for three forms of RTV 615:(1) the case in which the fresh mixture of resin and hardener was still in liquid form on the fused silica stage; (2) the case in which this mixture had hardened on the stage; (3) the case in which a block of previously formed solid RTV 615 was pressed onto the stage. Since our measurements only involved the solid material, only the latter two cases are considered here.

In Fig. 4 Frizzell's values are plotted, the point corresponding to case 2 in which the RTV 615 was hardened on the stage having the form △, and the point corresponding to case 3 in which the RTV 615 was pressed onto the stage having the form ▽. The hardened-on case agrees best with our results although the standard deviations are of the order of 15 or 20 m/s meaning that both agree rather well. (Estimates of standard deviations in speeds of sound and attenuation coefficients were done crudely using Frizzell's values for the standard deviations in the real and imaginary parts of the acoustic impedance and propagating errors ignoring cross correlations.) In our experiment considerable pressure (by hand) was applied during application of the RTV and it may be that we had better coupling to the fused silica resulting in better agreement with the (perhaps optimal) case of hardening the RTV onto the stage.

In Fig. 5 Frizzell's attenuation coefficients for RTV 615 are plotted for the hardened-on case (△) and for the pressed-on case (▽). Excellent agreement with our results exists. The standard deviations in Frizzell's values were estimated to be 1350 cm^{-1}. (See discussion in the paragraph immediately preceeding this one.)

For the cases of the tissues for which measurements are reported by Frizzell, mean values of speeds of sound and attenuation coefficients are given in Table 4.2 in Ref. 12, p. 65; in most cases standard deviations are also given in the table. In Figs. 8 and 9, Frizzell's values for dog muscle are plotted in triangles (△) and standard deviantions given. Remarkably good agreement is found not only with respect to mean values but with respect to standard deviations. An exception is our estimate of Frizzell's standard deviation of 14 000 cm^{-1} of the attenuation coefficient at 14 MHz; a value of 1400 cm^{-1} for this standard deviation would be consistent with our standard deviations in this frequency range. The present authors thought the value 14 000 cm^{-1}

TABLE II. Mean values for shear wave speeds of sound and attenuation coefficients for various materials for two different sets of measurements at 4.80 MHz. The repeat set of measurements were obtained following the first set after the source transducer A (see Fig. 1) had been removed and replaced on the mode conversion block. This was a reproducibility test.

Material	Mean value of shear wave speed of sound (m/s)			Mean value of shear wave attenuation coefficient (cm^{-1})		
	First set of measurements	Repeat set of measurements	% change	First set of measurements	Repeat set of measurements	% change
RTV 615	91.4	85.1	−7	1580	1600	+1
calfskin	60.9	67.3	+5	2200	1830	−18
animal hide gel without particles	25.4	27.3	+7	7130	9390	+27
TM liver (animal hide gel *with* particles)	19.6	24.5	+22	5960	7160	+18

might have resulted from a typographical error in Ref. 12; thus corresponding error bars were not introduced into Fig. 9.

In Figs. 12 and 13, Frizzell's mean values are given in triangles again. The points at 2.2 and 6.5 MHz are for dog liver and standard deviation bars are included. The point at 14 MHz corresponds to rat liver and no standard deviations were given by Frizzell. Again, the agreement between Frizzell's data and ours is very good. Notice particularly again the agreement of standard deviation ranges from relatively large values at the lower frequencies for the attenuation coefficients to very small values for the lower frequency range for speeds of sound.

C. Frequency dependencies

An overall perusal of the data in Figs. 3–15 shows the consistent tendency for both speeds of sound and attenuation coefficients to increase with frequency for all materials tested.

Using the relation $\mu = \omega^2\rho/k^2$ and the fact that $k_2 \equiv \omega/c_s + i\alpha_s$, one can solve for c_s and α_s in terms of μ_1, μ_2, ρ, and ω. These relations also appear on p. 40 of Ref. 12:

$$c_s = \left(\frac{(2\mu_1/\rho)[1 + (\omega\mu_2/\mu_1)^2]}{1 + [1 + (\omega\mu_2/\mu_1)^2]^{1/2}}\right)^{1/2} \tag{9}$$

and

$$\alpha_s = \left(\frac{-1 + [1 + (\omega\mu_2/\mu_1)^2]^{1/2}}{(2\mu_1/\rho)[1 + (\omega\mu_2/\mu_1)^2]}\right)^{1/2}. \tag{10}$$

As shown in Sec. IA, the real part, μ_1, of the complex shear modulus is the usual (static) shear modulus and the imaginary part is the negative of the product of the frequency, ω, and the coefficient of viscosity, μ_2. The coefficients μ_1 and μ_2 may depend on the frequency; however, it is interesting to take μ_1 and μ_2 to be independent of frequency and look for values of μ_1 and μ_2 giving an optimized fit to the data. What results is rather good agreement with the data over the whole range of frequencies. The dashed curves in Figs. 3–14 correspond to relations (9) and (10) above for c_s and α_s for the values of μ_1 and μ_2 given in Table I. An analysis for μ_1 and μ_2 values for the graphite-in-gelatin TM liver were not done because the data for this material were not significantly different from the case of plain gel.

Note in the table that the data for RTV 615 and calfskin produced similar values for μ_1 and μ_2 whereas data for the other tissues and the gel produced values of μ_2 which are an order of magnitude lower and of μ_1 which are more than an order of magnitude lower. Regarding μ_1, that for liver is essentially zero in distinction to the case for other tissues. Values of μ_1 and μ_2 for plain gel are both quite comparable to those for the muscle tissues.

Perhaps the best test of the idea that the shear wave properties of these materials can be described in terms of the constant values of μ_1 and μ_2 lies in the extent to which agreement between theory and experiment exists for RTV 615. (See Figs. 3–5.) Measurements on RTV 615 showed a relatively high degree of reproducibility. Considering Figs. 5 and 6 for speeds of sound, good agreement with the constant μ_1 and μ_2 model occurs for frequencies below about 7 MHz, but considerable disagreement exists above this frequency. Contrary to the situation for speeds of sound, disagreement dominates at the lower frequencies for the attenuation coefficients, the experimental values tending to be 50%–100% higher than the theoretical for frequencies below about 4 MHz.

VI. CONCLUSIONS

The extent of agreement between Frizzell's results and ours and the demonstrated reproducibility of our measurements constitutes strong evidence that these measurements are accurate within the limitations of the scatter in the data. The data promote the idea that the shear wave properties of the materials studied can be described in terms of relatively frequency-independent shear moduli (μ_1) and coefficients of viscosity (μ_2). However, the data also suggest that a degree of frequency dependence of the latter parameters does exist.

ACKNOWLEDGMENTS

The authors are most grateful to Colleen Schutz for the generation of the typescript and to Orlando Canto for the generation of the figures. This work was supported in part by NIH Grants R01-CA25634 and R01-GM30522.

[1] H. Pauly and H. P. Schwan, "Mechanism of Absorption of Ultrasound in Liver Tissue," J. Acoust. Soc. Am. 50, 692–701 (1971).

[2] R. L. Johnson, S. A. Goss, V. Maynard, J. K. Brady, L. A. Frizzell, W. D. O'Brien, Jr., and F. Dunn, "Elements of Tissue Characterization. Part I. Ultrasonic Propagation Properties," in NBS Special Publication 525: *Ultrasonic Tissue Characterization II*, edited by M. Linzer (U.S.GPO, Washington, DC, 1979), pp. 19–27.

[3] E. L. Carstensen, "Absorption of Sound in Tissues," in NBS Special Publication 525: *Ultrasonic Tissue Characterization II*, edited by M. Linzer (U.S.GPO, Washington, DC, 1979), pp. 29–36.

[4] W. J. Fry, Mechanism of Acoustic Absorption in Tissue," J. Acoust. Soc. Am. 24, 412–415 (1952).

[5] J. O'Donnell and J. G. Miller, "Mechanisms of Ultrasonic Attenuation in Soft Tissue," in NBS Special Publication 525: *Ultrasonic Tissue Characterization II*, edited by M. Linzer (U.S.GPO, Washington, DC, 1979), pp. 37–40.

[6] P. S. Epstein, and R. R. Carhart, "The Absorption of Sound in Suspensions and Emulsions. I. Water Fog in Air," J. Acoust. Soc. Am. 25, 553–565 (1953).

[7] J. R. Allegra and S. A. Hawley, "Attenuation of Sound in Suspensions and Emulsions: Theory and Experiments," J. Acoust. Soc. Am. 51, 1545–1564 (1972).

[8] E. L. Madsen, "Ultrasonically Soft-tissue-mimicking Materials," in *Medical Physics of CT and Ultrasound: Tissue Imaging and Characterization*, edited by G. D. Fullerton and J. A. Zagzebski (American Institute of Physics, New York, 1980), pp. 531–550.

[9] A. J. Barlow and J. Lamb, "The Visco-elastic Behavior of Lubricating Oils Under Cyclic Shearing Stress," Proc. R. Soc. London Ser. A 253, 52–69 (1959).

[10] A. J. Barlow, J. Lamb, A. J. Matheson, P. R. K. L. Padmini, and J. Richter, "Viscoelastic Relaxation of Supercooled Liquids. I," Proc. R. Soc. London Ser. A 298, 467–480 (1967).

[11] A. J. Barlow, A. Erginsav, and J. Lamb, "Viscoelastic Relaxation of Supercooled Liquids. II," Proc. R. Soc. London Ser. 298, 481–494 (1967).

[12] L. A. Frizzell, "Ultrasonic Heating of Tissues," Ph.D. thesis, University of Rochester, 1976.

[13] L. A. Frizzell, E. L. Carstensen, and J. F. Dyro, "Shear Properties of Mammalian Tissues at Low Megahertz Frequencies," J. Acoust. Soc. Am. 60, 1409–1411 (1976).

[14] RTV 615 is a silicone rubber compound manufactured by the General Electric Company.

[15]P. M. Morse, "Vibrations of Elastic Bodies; Wave Propagation in Elastic Solids," in *Handbook of Physics*, edited by E. U. Condon and H. Odishaw (McGraw-Hill, New York, 1967), pp. 3–99.
[16]R. T. Beyer and S. V. Letcher, *Physical Ultrasonics* (Academic, New York, 1969), pp. 30–33.
[17]Trade name for polymethyl methacrylate.
[18]Styrofoam is a trademark for rigid, lightweight, cellular polystyrene.
[19]G. W. C. Kaye and T. H. Laby, *Tables of Physical and Chemical Constants* (Longman, London, 1973).
[20]W. P. Mason, W. O. Baker, H. J. McSkimin, and J. H. Heiss, "Measurement of Shear Elasticity and Viscosity of Liquids at Ultrasonic Frequencies," Phys. Rev. 75, 936–946 (1949).
[21]E. L. Madsen, J. A. Zagzebski, and G. R. Frank, "Oil-in-gelatin Dispersions for Use as Ultrasonically Tissue-mimicking Materials," Ultrasound Med. Biol. 8, 277–287 (1982).
[22]P. R. Bevington, *Data Reduction and Error Analysis for the Physical Sciences* (McGraw-Hill, New York, 1969), pp. 59–60, particularly Eq. 4-9 on p. 60.
[23]I. A. Sokolnikoff and R. M. Redheffer, *Mathematics of Physics and Modern Engineering* (McGraw-Hill, New York, 1966), 2nd ed., p. 643.